RSC Advances

PAPER

View Article Online
View Journal | View Issue



Cite this: *RSC Adv.*, 2015, **5**, 51947

# Borneol-grafted cellulose for antifungal adhesion and fungal growth inhibition†

Bing Shi,‡[a] Di Luan,‡[a] Shihui Wang,[a] Lingyun Zhao,[b] Lei Tao,[c] Qipeng Yuan[a] and Xing Wang*[a]

Received 29th April 2015
Accepted 2nd June 2015

DOI: 10.1039/c5ra07894f

www.rsc.org/advances

Cellulose fibers modified to obtain antifungal activity have attracted much attention due to their versatile applications, although there are still some problems associated with the conventional protocols, including the toxicity to organisms, unwanted resistance, and gradually increasing environmental pressure. A natural and safe strategy is desired to design new types of antifungal cellulose. Herein, we present a borneol-grafted cellulose (BGC) by covalently tethering L-borneol, a natural product, to cellulose. The attained BGC has been characterized to confirm the chemical and amorphous features using a combination of spectroscopic and analytical techniques. This BGC material was subsequently challenged with *Mucor racemosus* and *Aspergillus niger*, and exhibited a remarkable performance in antifungal adhesion and fungal growth inhibition, suggesting the grafted borneol moieties are crucial for influencing the tactile sensing of fungal cells and subsequent selective inadhesion. The BGC has also been evaluated as a non-cytotoxic material, implying its great potential for biomedical and sanitary applications.

## 1. Introduction

Fungal contamination is one of the most troublesome issues causing adverse consequences in various fields such as biomedical devices, water storage and treatment systems, and food packing or processing equipment.[1–3] It is urgent in numerous areas to develop antifungal materials and surfaces to prevent/mitigate antifungal adhesion or colonization, or actively kill fungi on contact.[4] Great efforts have been made on this topic and many antifungal agents, such as immobilized antifungal drugs,[5] metals and their salts,[6,7] phenols,[8] and cationic compounds,[2,9] have been utilized to impart antifungal activity to the related materials. However, fungal cells (eukaryotes), rather than bacteria (prokaryotes), are more similar to mammalian cells in terms of metabolism processes and cellular structure, which may usually result in direct toxicity to mammalian cells from the antifungal activity. Now, more and more problems have been arising during practical applications of conventional antifungal agents, in particular, their toxicity to organisms, unwanted resistance, and gradually increased environmental pressure.[10–12] Therefore, new strategies for the development of safe antifungal materials are still highly desired.[2]

Ideal antifungal materials or surfaces should be biocompatible and environment-friendly. Thus, the application of natural antimicrobials has been recognized as a suitable strategy with the popular environmental protection movement. As one of the most studied and excellent natural materials,[13,14] cellulose fiber has been employed in broad fields, including textiles,[15] food packing,[16] medical accessory materials,[17] and the environmental domain.[18] Meanwhile, cellulose is also known as a good culture material for microorganisms, owning to its large surface area and moisture absorbability. For safety reasons, the antifungal issue must be considered for cellulose fibers, especially in biomedical and healthcare areas.[19] Natural compositions including chitosan,[20] natural dyes,[21] and essential oils[22] have been used to modify cellulose fibers and demonstrated promising results. However, most of the current applied natural materials still mainly depend on their poisoning effect on the cells or disrupting the integrity of cell membranes to act as antimicrobials, which hamper the application of those natural materials in broader fields.

As a broad-spectrum defensive strategy to prevent antifungal adhesion, utilizing of the "tactile sense" of fungal cells to prevent their adhesion in the initial phase has not been extensively studied. Our recent work has demonstrated that the cells

[a]*The State Key Laboratory of Chemical Resource Engineering, Beijing University of Chemical Technology, Beijing 100029, P. R. China. E-mail: wangxing@mail.buct.edu.cn*

[b]*Key Laboratory of Advanced Materials, Ministry of Education, Institute of Regenerative Medicine and Biomimetic Material Science and Technology, Tsinghua University, Beijing 100084, P. R. China*

[c]*The Key Laboratory of Bioorganic Phosphorus Chemistry & Chemical Biology (Ministry of Education), Department of Chemistry, Tsinghua University, Beijing 100084, P. R. China*

† Electronic supplementary information (ESI) available: Detailed experimental description and results including EDS, XRD, ChemBioDraw simulation, antifungal evaluation, *etc.* See DOI: 10.1039/c5ra07894f

‡ These authors equally contributed to this work.

exhibited a distinct inclination towards different chiral stereochemistry during their adhesion on external surfaces,[23,24] which inspired us to make further efforts in developing antimicrobial materials or surfaces catering to the "chiral taste" of microbe cells. A model system using polyborneolacrylate was thus achieved,[25] where an L-borneol containing polymer with good biocompatibility was proven to be a promising candidate for bacterial adhesion inhibition. As a well-known safe and common natural product, L-borneol is suitable for use based on the natural strategy for endowing antimicrobial activity to cellulose. In the current study, a borneol-grafted cellulose (BGC) has been synthesized for the first time by covalently tethering L-borneol onto the cellulose surface (Scheme 1). The antifungal activity of the modified cellulose has been systematically studied, demonstrating a remarkable performance in antifungal adhesion and fungal growth inhibition. Considering the excellent and general antimicrobial effect and that L-borneol is safe, easily available and biocompatible, this BGC composite might have potential to be used as a new generation antifungal material in the medical and clinical fields.

## 2. Experimental section

### 2.1. Materials

Cellulose (Sigma, powder, dry loss <5%), L-borneol (J&K, 99%), chloroacetyl chloride (SCR, 99%), and 1-butyl-3-methylimidazolium acetate ([BMIm]Ac, Lanzhou Green-chem ILS, 98.5%) were used as received. Pyridine, tetrahydrofuran (THF) and triethylamine (TEA) were used after a dehydration treatment with molecular sieves.

### 2.2. Preparation and characterization of the BGC

Sodium hydroxide (0.7 g) was dissolved in 80% ethanol solution. Cellulose (0.8 g) was treated with 10 mL of the as-prepared solution at room temperature for 24 h. After washing with distilled water and drying under vacuum, the alkali cellulose was obtained as a white solid with a yield of 82%. Then, 0.2 g of alkali cellulose was dissolved in 10 mL of [BMIm]Ac at 90 °C for 2 h and the solution was adjusted to pH 8 by adding TEA, followed by addition of chloroacetyl-L-borneol (CAB, 0.6 g, 2.6 mmol, the synthetic method for CAB is shown in the ESI†). The solution was then kept stirring at 70 °C for 3 days. The product was precipitated from the [BMIm]Ac system with diethylether and washed by Soxhlet extraction with ethanol (100 mL) for 2 days to remove impurities. Finally, purified BGC was obtained as a white solid with a yield of 93.8%. It was characterized using a combination of Fourier transform infrared spectroscopy (FT-IR), $^{13}C$ nuclear magnetic resonance spectroscopy ($^{13}C$ NMR), X-ray photoelectron spectroscopy (XPS), energy-dispersive X-ray spectroscopy (EDS), and X-ray diffraction (XRD).

### 2.3. Antifungal activity assay

*Mucor racemosus* (*M. racemosus*) and *Aspergillus niger* (*A. niger*) were used in this study. Typically, the fungus was aerobically grown for 5 days on beef extract peptone solid medium in an electro-heating standing-temperature cultivator at 37 °C. Then a small amount of fungal cells were taken out using an inoculating loop and diluted in a 0.9% saline (1 mL). The culture was used as the fungal suspension for the antifungal experiments.

To evaluate the antifungal adhesion activity of the BGC sample, the BGC powder was pressed into 13 mm diameter sized pellets, where cellulose was used as a control for the same test. The two kinds of pellets were individually affixed onto the same beef extract peptone solid medium and then, 10 μL of fungal solution was dropped in the center of the plate, by controlling the distance to the test samples. The plate was aerobically cultured at 37 °C in an electro-heating standing-temperature cultivator. The fungi were allowed to grow and expand from the medium center to the pellet surface. Fungal growth at different periods was observed and recorded with a camera.

Scanning electron microscopy (SEM, Hitachi S-4700) was used to study the morphologies of fungal cells on the sample surface. The aforementioned samples were immobilized with 2.5% glutaraldehyde for 2 h at 4 °C. The fungal cells were dehydrated using 50, 60, 70, 80, 90 and 100% ethanol for 10 min, respectively. The samples were freeze-dried for 12 h prior to SEM observation.

### 2.4. *In vitro* investigation of the biocompatibility of the BGC by MTT assay

The biocompatibility of the material was investigated with L929 mouse fibroblast cells (purchased from Cell Resource Center,

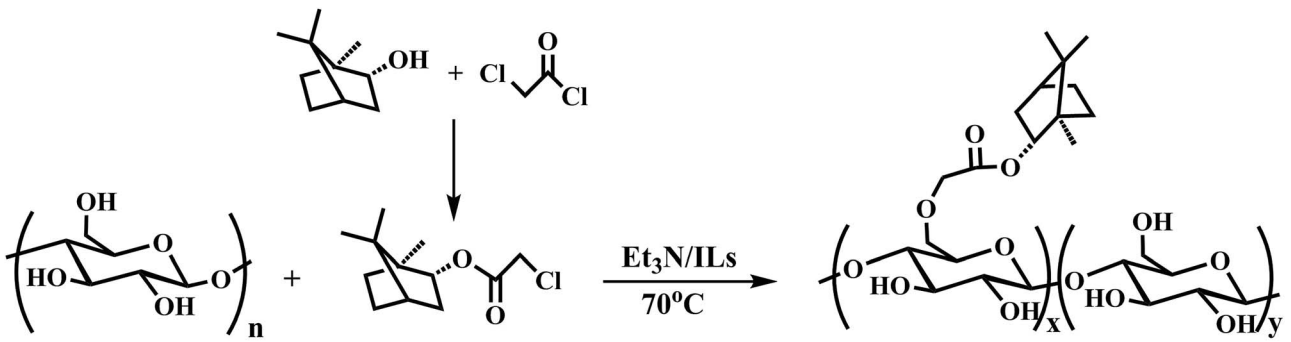


Scheme 1 Synthesis of chloroacetyl-L-borneol (CAB) and subsequently grafting to cellulose to obtain the borneol-grafted cellulose (BGC) *via* an etherification method.

 

IBMS, CAMS/PUMC, Beijing, China). Cells at the logarithmic growth phase were adjusted to a concentration of $8 \times 10^5$ cells per mL in a complete medium (CM), which was composed of 90% RPMI-1640 medium, 10% fetal bovine serum (FBS) and 1% antibiotics (100 units per mL penicillin and 100 units per mL streptomycin). Then the cell suspension was added into a 96-well plate (100 μL per well) and incubated for 24 h at 37 °C under the air conditions of 5% (v/v) $CO_2$. Meanwhile the prepared BGC was soaked with RPMI-1640 medium (0.2 g $mL^{-1}$) for 24 h and the impregnation solution was centrifuged to replace the CM solution in the plate ($n = 9$). The same procedure was performed on cellulose as a negative control. After 48 h of incubation, cell viability was determined using a MTT Assay Kit based on the manufacturer's instructions. The relative growth rate (RGR) of the cells was calculated according to the following formula: RGR = $Abs_{490}$ test/$Abs_{490}$ control × 100%. Finally, the toxicity grade was assessed on the basis of the RGR. The MTT assay of the borneol molecules was partially different. Borneol was firstly dissolved in dimethyl sulfoxide (DMSO). A dilution of borneol (15 μg $mL^{-1}$) was made in CM solution with the final concentration of DMSO below 0.5%. This DMSO content had no influence on cell growth based on preliminary experiments. Then the MTT assay was operated with the same method.

## 3. Results and discussion

### 3.1. Synthesis and characterization of the BGC

BGC was synthesized by grafting CAB onto cellulose as shown in Scheme 1. In the first step, CAB was synthesized, endowing the borneol molecule with a lively halogen substituent.[26,27] Then, CAB reacted with the 6-hydroxyl group of cellulose to produce the BGC *via* an etherification reaction[26–29] in ionic liquid [BMIm]Ac, which could improve the solubility of the cellulose. The synthesized BGC was characterized by combining measurements from FT-IR, NMR, XPS and EDS. The grafting ratio of the BGC was then denoted. Moreover, the internal structural information was revealed by XRD measurements.

The reaction occurrence was first assessed using FT-IR. Fig. 1(a) shows typical spectra of the BGC sample and the cellulose. A significant peak at 1727 $cm^{-1}$, corresponding to the C=O stretching of the ester, was detected in the BGC sample, indicating the grafting of CAB onto cellulose. Consequently, an increased vibration peak at 2962 $cm^{-1}$, which corresponds to the C–H stretching of methyl or methylene groups was noticed in the spectral characteristics of the borneol pendants. Meanwhile, compared with the peaks of the cellulose sample, the BGC sample yielded a new peak at 1190 $cm^{-1}$, corresponding to the signal of C–O–C stretching of the linking groups resulting from the etherification reaction, thus confirming the successful grafting of borneol onto cellulose. In addition, all of them were characterized with a dominant O–H stretching vibration (3070–3570 $cm^{-1}$), C–H stretching vibration (2960 $cm^{-1}$) and C–O stretching vibration (1029 $cm^{-1}$) because of the presence of basic glucose units.

More visual evidence was supplied by $^{13}C$ NMR detection. Fig. 1(b) shows the analyzed results of the $^{13}C$ NMR spectra of the final BGC product and the control groups of cellulose and CAB molecules. In comparison with the cellulose's spectrum that is marked with band a, b, and c for the typical carbon groups, the BGC sample exhibited two remarkable signals located at $\delta$ 20 ppm (band d) and $\delta$ 173 ppm (band f), which could be attributed to methyl/methylene and ester groups, respectively. Meanwhile, the signal of the ether linkage (C–O–C) was found at $\delta$ 68.3 ppm (band e). $^{13}C$ NMR detection of the CAB molecules showed three key bands located at $\delta$ 41.3, 167.5, and 80.7 ppm. The carbon near the halogen (C–Cl) contributed a band g at $\delta$ 41.3 ppm, which had disappeared on the BGC's spectrum as expected. While, another two key bands (k and l) could be also found in the BGC's spectrum rather than the cellulose's spectrum, demonstrating a proper BGC structure.

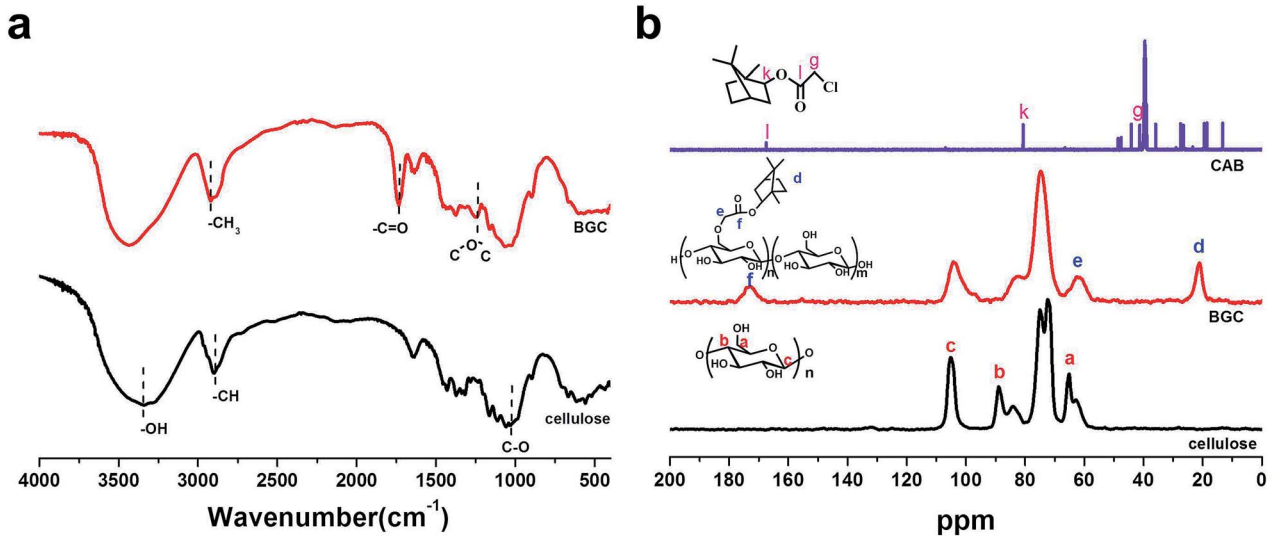


Fig. 1 (a) FT-IR spectra of BGC (top) and cellulose (bottom). (b) $^{13}C$ NMR spectra of cellulose (bottom), BGC (middle) and CAB (top).

The XPS spectra (Fig. 2) provided further proof for the grafting of CAB onto cellulose. For the BGC sample, the C 1s signal showed a new peak located at 283 eV that corresponds to the C–C/C–H groups of borneol. Whereas, no signal of Cl elements was found at the range of 197–202 eV,[30] which was in agreement with the NMR measurements. Quantitative analysis for borneol grafting was performed using EDS measurements (Fig. S1 in ESI†), which demonstrated the elemental content of the BGC sample. It is well known that cellulose is formed from repetitive glucose units and borneol is mainly composed of carbon elements. Therefore, the grafting rate could be calculated based on the changing of the C/O element ratio. After borneol grafting, the C/O ratio in BGC (C: 52.77 wt%, O: 47.23 wt%) was increased to 1.12 compared with the ratio of 0.89 for cellulose (C: 47.13 wt%, O: 52.87 wt%). With the help of a ChemBioDraw simulation program (see Fig. S2 in ESI†), the borneol-grafting rate was calculated to be approximately 17%, in other words, every six glucose units had one CAB molecule. In addition, no signal of Cl elements was detected at 2.1269 kV.

As the cage structure of borneol was grafted onto cellulose, changes in the internal crystallinity were studied using XRD observations. Fig. S3 in the ESI† shows the full XRD patterns of the samples before and after the borneol grafting onto cellulose. The typical peaks of cellulose at $2\theta = 14.5^\circ$, $16.0^\circ$, $22.5^\circ$ represented the 101, $10\bar{1}$, 002 diffraction planes respectively, corresponding to cellulose I. After borneol grafting, wide deformation was observed mainly due to two distinct reasons. Firstly, cellulose dissolved and precipitated in the ionic liquid, resulting in a crystal structure change. More importantly, borneol is a bicyclic monoterpene and this cage molecule caused the macromolecular structure to be disordered.

### 3.2. Antifungal adhesion assay

The antifungal adhesion activity of the prepared BGC sample against *M. racemosus* was investigated and is shown in Fig. 3, where BGC and cellulose pellets were put into the same plate with solid medium culturing *M. racemosus* in the central location. After 2 days, *M. racemosus* grew to the edge of the pellets and started to attack the pellets. A significant phenomenon was observed after 4 days of incubation. The cellulose pellet was gradually covered with *M. racemosus* cells as a distinct frontier (pink arrow in Fig. 3) could be visualized on the surface, but on the BGC surface, no *M. racemosus* cells adhered or grew on it. Even after 8 days, the BGC sample displayed perfect antifungal activity, exhibiting a clear surface without any fungal strains. It thus could be concluded that the BGC material revealed a superb performance in inhibiting *M. racemosus* cell adhesion and growth on it.

To investigate the adhesion details, SEM measurements were carried out to study the morphologies of *M. racemosus*. Fig. 4 shows the SEM images of the fungal cell adhesion on the above-mentioned pellets. A large amount of grown sporangia and hypha were found on the cellulose surface (Fig. 4a) and a lively germination of spores was exhibited therein (Fig. 4a′ and the inset). On the other hand, on the BGC surface (Fig. 4b), only a few hyphae could be observed near the boundary and the serendipitous spores stayed near the hypha presenting a whole sphericity (Fig. 4b′), indicating a growth inhibition of spores on the BGC surface. At least, these phenomena demonstrated the success of the cellulose modification and the high antifungal power of the grafted borneol molecules. It is obvious that the grafting ratio of the borneol of BGC could affect the antifungal activity. But to our surprise, the antifungal activity of BGC is achieved with a relatively low grafting rate (17%) of borneol pendants as proven in the above-mentioned analysis. As

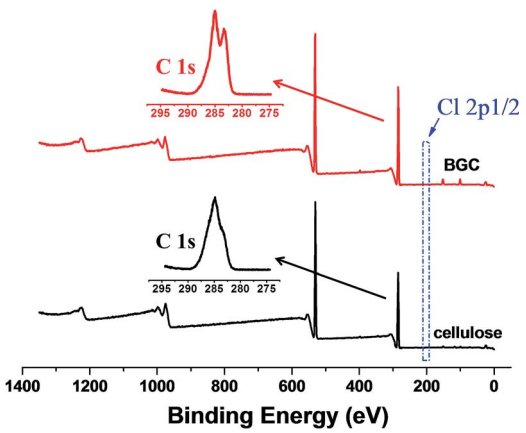


Fig. 2 XPS measurements of BGC (top) and cellulose (bottom). The inset spectra are obtained from the C 1s. The new peak located at 283 eV for the BGC sample corresponds to the C–C/C–H groups of borneol. No signal of Cl elements was found at the range of 197–202 eV, which could rule out the possibility of a mixture of CAB and cellulose, thus indicating a successful grafting of CAB onto cellulose.

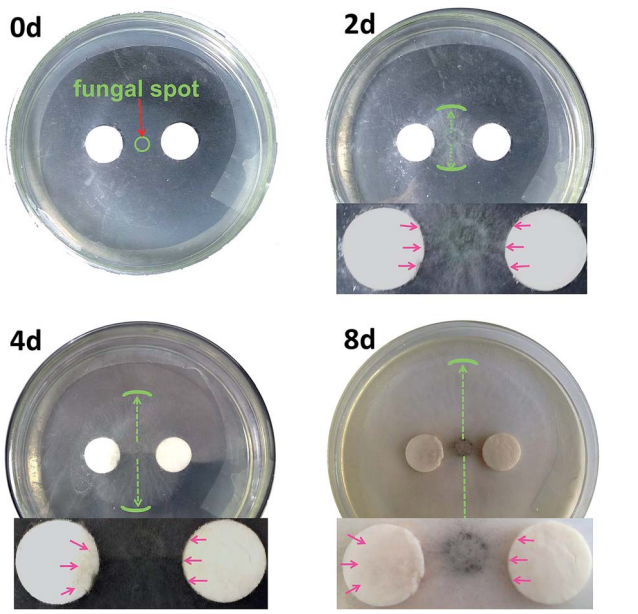


Fig. 3 Study of the antifungal adhesion activity of cellulose (left) and BGC (right) pellets, by culturing *M. racemosus* in the central location of the solid medium, in the same plate for different periods of time. The results of 0, 2, 4 and 8 days are shown here. The insets exhibit an enlarged image. Pink arrow: the growth frontier of *M. racemosus* on the pellets. Green circle: the range of the inoculated *M. racemosus* spot. Green arc: the growth range of *M. racemosus*.

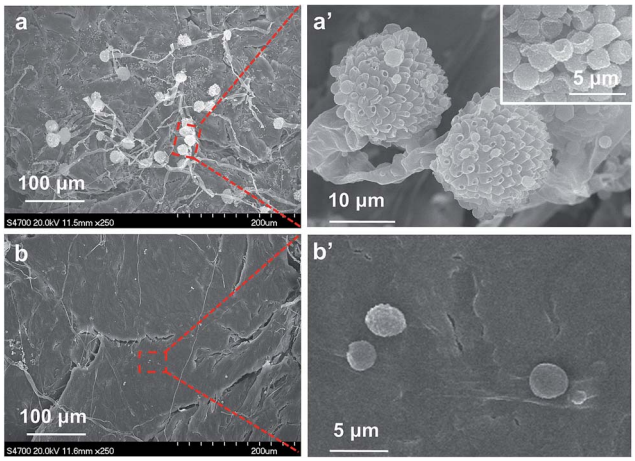


Fig. 4 SEM images of the antifungal adhesion results for the cellulose (a, a′) surface and the BGC (b, b′) surface. By comparison, a distinct antifungal adhesion inhibition could be found after grafting borneol molecules onto cellulose.

expected, if the grafting ratio of borneol decreased to approximately 6.2% (Fig. S4 in ESI†), a lesser antifungal effect could be observed (Fig. S5 in ESI†).

As mentioned, the grafting of L-borneol on cellulose was realized by employing a short acetyl linker. It is not consistent with the offensive strategy, where surface-tethered antifungal agents need to have a deep range of penetration afforded by longer anchoring linkers in order to reach the fungal cell membrane, considering the thickness of the outer protective fungal envelope (~100 nm).[2] Therefore, the interaction should happen on the outside of the fungal envelope. According to the aforementioned phenomena, we could find that the BGC mainly performs a defensive antifungal effect. Based on the understanding that cells could distinguish stereochemical signals of external surfaces,[23–25] we deduced that a biological surface recognition may be a probable explanation for the antifungal action of our BGC sample. In other words, fungal cells recognized the caged bicyclic borneol molecules and subsequently tended to inadhesion on the BGC surface, where borneol grafting plays the key role in the antifungal effect of the BGC product.

In order to further demonstrate the antifungal properties, we subsequently performed the experiment with *A. niger*. Considering that the BGC is an antifungal pellet, the operation was carried out in ambient conditions. After 8 days of incubation, a clear surface with a distinct boundary was found for the BGC pellet (Fig. 5), while the cellulose pellet was covered with dense *A. niger* cells. To our surprise, other fungi such as *M. racemosus* and *yeast* that might come from the environment were found in the plate, but more importantly, the *yeast* cells did not tend to adhere to the BGC pellet. Through careful checking under a microscope (Fig. 5, the insets a, b and c), only a few *A. niger* cells were found at the boundary of the BGC pellet, but their amount was much less compared with the cellulose pellet. Based on the aforementioned mechanism, we speculated that the appearance of those cells was not due to the active adhesion of fungal cells. In any case, these phenomena distinctly exhibited a conversion of the antifungal activity from the surrender of cellulose to the resistance of BGC.

### 3.3. *In vitro* biocompatibility evaluation

A standard MTT assay showed that the BGC material was non-cytotoxic to L929 cells (Fig. 6). The relative growth rate (RGR) of the BGC sample was found to be similar to that of cellulose. In addition, the RGR of the borneol molecules was confirmed to be nontoxic at the employed concentration (15 μg $mL^{-1}$), which has also been proven in previous literature.[31] Since the borneol molecules were grafted onto cellulose with covalent bonds, the

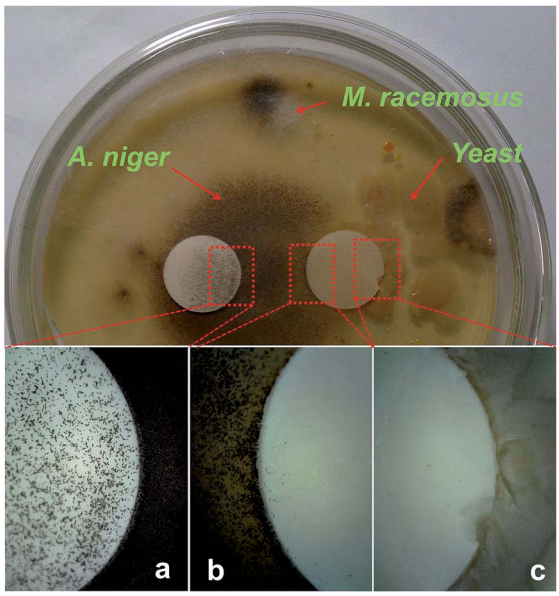


Fig. 5 Antifungal adhesion activity of pellets of cellulose (left) and BGC (right) by culturing *A. niger* for 8 days. The operation was carried out in ambient conditions, thus *M. racemosus* and *yeast* strains were also found. Optical micrographs showed that the fungal cells adhered to the cellulose pellet (inset a) and stopped adhering to the BGC pellet (inset b and c).

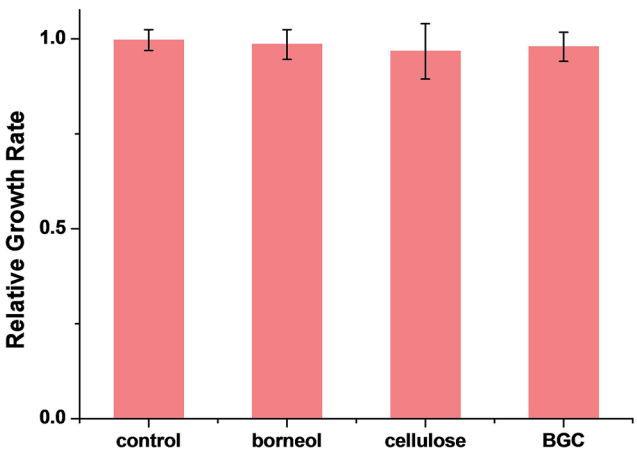


Fig. 6 MTT results of the RGR of L929 cells for 2 days of incubation in BGC conditioned media. The data are presented as the mean plus or minus the standard deviation ($n$ = 9 for each group).

Table 1 MTT results for the borneol, cellulose and BGC

| Sample | Days of culture | Relative growth rate (%) | Toxicity grade |
|---|---|---|---|
| Control | 2 | 99.71 ± 2.75 | 1 |
| Borneol | 2 | 98.53 ± 3.93 | 1 |
| Cellulose | 2 | 96.75 ± 7.29 | 1 |
| BGC | 2 | 97.95 ± 3.84 | 1 |

BGC material should be stable to a certain degree. Therefore, the above-mentioned concentration is suitable for the MTT assay. As a result, these assays demonstrated that the borneol grafting did not introduce any toxicity into the cellulose material. According to the standard toxicity rating, the cell toxicity of all the test materials was in grade 1 (Table 1), indicating no toxicity in the framework of safety for use.

## 4. Conclusions

In summary, borneol grafting onto cellulose is presented, employing chloroacetyl chloride as a covalent linking agent and a two-step reaction. A grafting ratio of approximately 17% was realized. Although the grafting ratio was relatively low, the BGC material displayed a remarkable performance in antifungal adhesion and fungal growth inhibition. Thus, this novel BGC material can be considered as one candidate for antifungal celluloses. More importantly, both borneol and cellulose are natural products, suggesting an advanced natural strategy for exploiting cellulose's potential use in antifungal adhesion and colonization. The simple modification of adding small borneol molecules onto cellulose not only resulted in a significant conversion of the interfacial antifungal property, but also opened a new avenue for developing a new generation of antimicrobial celluloses. This environment-friendly material will advance potential applications in the fields of the biomedicine, textile and food industry.

## Acknowledgements

The authors thank the National Natural Science Foundation of China (21204004), the Beijing Natural Science Foundation (2132040), the Specialized Research Fund for the Doctoral Program of Higher Education (20120010120011), and the Fundamental Research Funds for Central Universities of China (YS1407) for their funding support.

## Notes and references

1 P. Li, Y. F. Poon, W. F. Li, H. Y. Zhu, S. H. Yeap, Y. Cao, X. B. Qi, C. C. Zhou, M. Lamrani, R. W. Beuerman, E. T. Kang, Y. G. Mu, C. M. Li, M. W. Chang, S. S. J. Leong and M. B. C. Park, *Nat. Mater.*, 2011, **10**, 149–156.
2 B. R. Coad, S. E. Kidd, D. H. Ellis and H. J. Griesser, *Biotechnol. Adv.*, 2014, **32**, 296–307.
3 S. P. Hudson, R. Langer, G. R. Fink and D. S. Kohane, *Biomaterials*, 2010, **31**, 1444–1452.
4 T. Segura, A. M. Puga, G. Burillo, J. Llovo, G. Brackman, T. Coenye, A. Concheiro and A. C. Lorenzo, *Biomacromolecules*, 2014, **15**, 1860–1870.
5 C. S. O. Paulo, M. Vidal and L. S. Ferreira, *Biomacromolecules*, 2010, **11**, 2810–2817.
6 R. Prucek, J. Tuček, M. Kilianová, A. Panácek, L. Kvítek, J. Filip, M. Kolár, K. Tománková and R. Zboril, *Biomaterials*, 2011, **32**, 4704–4713.
7 B. Jia, Y. Mei, L. Cheng, J. Zhou and L. Zhang, *ACS Appl. Mater. Interfaces*, 2012, **4**, 2897–2902.
8 L. Yu, G. H. Ling, X. M. Deng, J. Jin, Q. Jin and N. Guo, *Antimicrob. Agents Chemother.*, 2011, **55**, 3609–3612.
9 F. X. Hu, K. G. Neoh, L. Cen and E. T. Kang, *Biotechnol. Bioeng.*, 2005, **89**, 474–484.
10 P. V. Asharani, Y. L. Wu, Z. Y. Gong and S. Valiyaveettil, *Nanotechnology*, 2009, **19**, 255102.
11 M. Ahamed, R. Posgai, T. J. Gorey, M. Nielsen, S. M. Hussain and J. J. Rowe, *Toxicol. Appl. Pharmacol.*, 2010, **242**, 263–269.
12 P. V. Asharani, G. L. K. Mun, M. P. Hande and S. Valiyaveettil, *ACS Nano*, 2008, **3**, 279–290.
13 S. H. Ye, J. Watanabe, M. Takai, Y. Iwasaki and K. Ishihara, *Biomaterials*, 2006, **27**, 1955–1962.
14 P. S. Liu, Q. Chen, X. Liu, B. Yuan, S. S. Wu, J. Shen and S. C. Lin, *Biomacromolecules*, 2009, **10**, 2809–2816.
15 H. Krizova and J. Wiener, *Autex Res. J.*, 2013, **13**, 33–36.
16 X. Luo and L. Zhang, *Food Res. Int.*, 2013, **52**, 387–400.
17 B. N. Chukwumezie, M. Wojcik, P. Malak and M. C. Adeyeye, *AAPS PharmSciTech*, 2002, **3**, 10–22.
18 E. Feese, H. Sadeghifar, H. S. Gracz, D. S. Argyropoulos and R. A. Ghiladi, *Biomacromolecules*, 2011, **12**, 3528–3539.
19 S. H. Wang, R. L. Niu, H. S. Jia, L. Q. Wei, J. M. Dai, X. G. Liu and B. S. Xu, *Bull. Mater. Sci.*, 2011, **34**, 629–634.
20 L. F. Zemljič, Z. Peršin and P. Stenius, *Biomacromolecules*, 2009, **10**, 1181–1187.
21 R. Singh, A. Jain, S. Panwar, D. Gupta and S. K. Khare, *Dyes Pigm.*, 2005, **66**, 99–102.
22 L. Jing, Z. T. Lei, L. Li, R. J. Xie, W. P. Xi, Y. Guan, L. W. Sumner and Z. Q. Zhou, *J. Agric. Food Chem.*, 2014, **62**, 3011–3033.
23 X. Wang, H. Gan, T. L. Sun, B. L. Su, H. Fuchs, D. Vestweber and S. Butz, *Soft Matter*, 2010, **6**, 3851–3855.
24 X. Wang, H. Gan, M. X. Zhang and T. L. Sun, *Langmuir*, 2012, **28**, 2791–2798.
25 L. Luo, G. Li, D. Luan, Q. Yuan, Y. Wei and X. Wang, *ACS Appl. Mater. Interfaces*, 2014, **6**, 19371–19377.
26 X. Wang, H. Gan and T. Sun, *Adv. Funct. Mater.*, 2011, **21**, 3276–3281.
27 A. E. Idrissi, S. E. Barkany, H. Amhamdi and A. K. Maaroufi, *J. Appl. Polym. Sci.*, 2013, **127**, 3633–3644.
28 S. Vogt, D. Klemm and T. Heinze, *Polym. Bull.*, 1996, **36**, 549–555.
29 I. Erol, Z. Şahin and L. Özcan, *Polym. Eng. Sci.*, 2013, **53**, 1383–1393.
30 G. Chamoulaud and D. Bélanger, *Langmuir*, 2004, **20**, 4989–4995.
31 J. Y. Hur, S. C. Pak, B. S. Koo and S. Jeon, *Pharm. Biol.*, 2013, **51**, 30–35.

 